Journal of Chemical Science and Engineering
JCSE, 3(3): 138-146
www.scitcentral.com

ISSN: 2642-0406

Original Research Article: Open Access

Experimental and Computational Chemistry Studies on Decolouration of Water Polluted by Neutral Red Dye by Adsorption unto Wood Saw Dust

Anduang Ofuo Odiongenyi*

*Department of Chemistry, Akwa Ibom State University Ikot Akpaden, Mkpat Enin Local Government Area, Akwa Ibom State, Nigeria.

Received April 10, 2020; Accepted May 12, 2020; Published May 14, 2020

ABSTRACT

In attempt to investigate the possibility of decolorizing water polluted by neutral red dye, wood saw dust was selected as a cheap raw material for the adsorption of the dye from aqueous solution. Batch adsorption method was used to investigate the effect of concentration of the dye, adsorbent dosage, period of contact and temperature. Concentration of the dye was determined using an ultraviolet-visible spectrophotometer. Results obtained indicated that wood saw dust has the potential removal efficiency in the range of 85 to 91 % (which corresponded to equilibrium adsorption concentration of 6.42 to 13.25 mg/g respectively). Adsorption of the dye increased with increase in concentration. Also, within some respective certain critical points, the adsorption of the dye was also observed to increase with increase in the period of contact, temperature and adsorbent dosage. The adsorption of the dye agreed with Langmuir, Temkin and Dubinin-Raduskevich isotherms. Calculated thermodynamic and other data indicated that the adsorption of neutral red dye is also spontaneous and supports the mechanism of chemisorptions. A pseudo second order kinetic and intra particle diffusion models were also obeyed by the adsorption data. Computational chemistry Fukui function and molecular orbital analysis indicated that the site for the adsorption of the dye is through the pyridine nitrogen bond of the dye. This proposed electron donation site was supported by Huckel charge analysis, MM2 simulation and HOMO and LUMO profiles. Regeneration experiment indicated that 68 % of the adsorbent was restored.

Keywords: Water pollution, Dye, Remediation, Adsorption, Wood sawdust

INTRODUCTION

Clean water is highly needed for various industrial, natural and domestic purposes. One of the major requirements is that the water must be colorless and free from toxic content [1]. Dyes of various forms have been identified as the commonest source of color pollution to our water system. Sources of dyes pollution may include textile industries, ternary industries, some manufacturing industries, paint industries and chemical laboratories [2].

Some dyes have been confirmed to be toxic, indicating that they can be poisonous when present in significant concentration. In view of this, several studies have been reported on the removal of different dyes using adsorption and other techniques. Adsorption technique has proven to be economical, eco-friendly and one of the best methods [3]. The use of wood or timber waste for the adsorption of dyes has been reported for a number of dyes [4]. The use of some materials to remove dyes from aqueous solution has been reported. For example,

- Use of bentonite to remove methylene dye from aqueous solution [5]
- Use of clay and modified clay to adsorb some dyes from aqueous solution [6]
- Use of some adsorbents to remove some dyes from aqueous solution and found that some plant materials are excellent materials for the removal of some dyes from aqueous solution [7]
- Use of clay-based materials for the adsorption of some dye and reported excellent adsorption efficiency [8]

Corresponding author: Anduang Ofuo Odiongenyi, Department of Chemistry, Akwa Ibom State University Ikot Akpaden, Mkpat Enin Local Government Area, Akwa Ibom State, Nigeria, Email: anduangodiong@gmail.com

Citation: Odiongenyi AO. (2020) Experimental and Computational Chemistry Studies on Decolouration of Water Polluted by Neutral Red Dye by Adsorption unto Wood Saw Dust. J Chem Sci Eng, 3(3): 138-146.

- Natural clay is found to be a good adsorbent for some cationic and anionic dyes [9]
- Use of some plant materials for the removal of some cationic and anionic dyes [7]
- Studies on the removal of neutral red dye by adsorption process have been reported for cationic neutral red dye using rice husk [10]
- Use of nano materials to remove neutral red dye from aqueous solution through adsorption [11]
- Fe_3O_4-nanospheres and pyrolytic char used to remove neutral red dye from aqueous solution using adsorption mechanism [12-14]

The present study is aimed at using saw dust of *musanga cecropioides*to remove neutral red dye from aqueous solution.

Batch adsorption process is used in this study. The study shall be supported by computational chemistry, which is aimed at finding the possible adsorption site through Fukui function calculations. Knowledge of mechanism of adsorption can provide a clue to future study of possible remediation measures. The chemical structure of NR dye is shown in **Figure 1.**

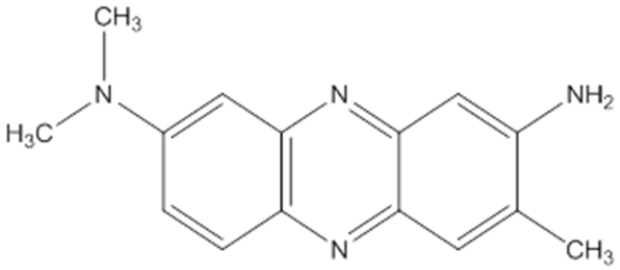

Figure 1. Chemical structure of dye.

The chemical name for the compound is N^7, N^7, 7-trimethylphenazine-2, 8-diamine. The compound contains hetero atoms; it is aromatic and has functional groups suitable for adsorption.

MATERIALS AND METHODS

Batch adsorption process as reported elsewhere was used to study the effect of concentration, contact time, adsorbent dosage and temperature [15]. Equilibrium concentration of the dye was calculated using equation 1[5]

$$q_e = \frac{C_0 - C_e}{C_0} \times \frac{V}{m} \quad (1)$$

Where C_0 is the initial concentration of the dye, C_e is the equilibrium concentration of the dye, V is the volume of solution and m is the mass of the adsorbent. Computational chemistry calculations were performed using DFT method in Hyper Chem package. Full geometry optimization was achieved using AMBER method of MM method in the same Hyper Chem package. Molecular mechanics (MM) simulation was done using MM2 package in the ChemBio 2018. ChemBio 2018 was also used to developed graphic for input into hyperChem and MM calculations.

RESULTS AND DISCUSSIONS

Batch adsorption study

Beer-Lambert law which proposes a linear relationship between absorbance and concentration according to the equation 2,

$$A = \in lC \quad (2)$$

Where A is the absorbance, εis the absorptivity, l is the path length and C is the concentration of the dye. The equation suggests a linear plot (with zero intercept) when values of absorbance are plotted against concentrations. The above model was used to develop a calibration curve through which concentrations of the dye were obtained by extrapolation. In this study, effect of concentration, period of contact, pH and particle size on adsorption of NR dye were investigated. **Figure 2** shows variation of equilibrium concentration of NR dye adsorbed with concentration. It is observed in the plot that the amount of NR adsorbed increases with increase in concentration which implies that increase in the amount of NR molecules diffusing onto the adsorbent also favors increase in the rate of adsorption.

The amount of dye adsorbed was also found to vary with adsorbent dosage as shown in **Figure 3**. The equilibrium concentration of NR adsorbed, first increased with increase in adsorbent dosage up to a critical point, beyond which, the amount adsorbed started decreasing with increase in adsorbent dosage. The observed trend suggests that the number of adsorption sites might have increase with increase in the amount of adsorbent, thus giving ways for adsorbate to stick to the surface until maximum amount of adsorbate had been adsorbed. It is also possible that diffusion rate of adsorbate unto the adsorbate decreases after the critical point since much of the adsorbate's molecules had already been adsorbed. Also, at this point, desorption can set in or there may be no significant increase in the number of adsorbate molecule.

Figure 4 reveals the pattern obtained for the variation of the amount of NR dye adsorbed with time. From the plot, it is evident that the equilibrium amount of NR dye adsorbed by wood saw dust increases with increase in the period of contact until it approaches a maximum, after which further increase in time did not increase the amount of dye adsorbed. Given a fixed amount of adsorption site and concentration of adsorbent, the more the adsorbate solution remains in contact with the adsorbent, probability of adsorption will increase but at a maximum, most of the adsorption sites have been occupied. Consequently, provided there is no desorption, then the amount NR dye adsorbed will increase with time and then remain constant.

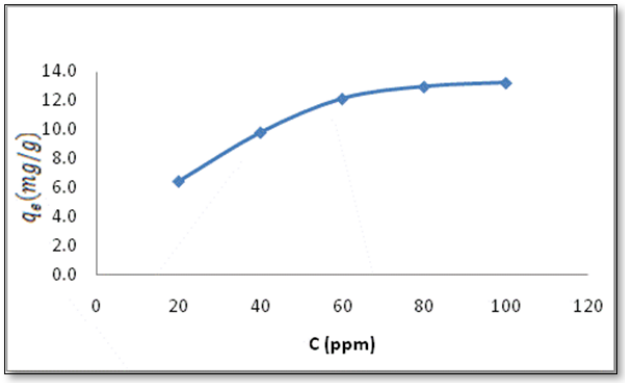

Figure 1. Variation of the amount of NR dye adsorbed with time

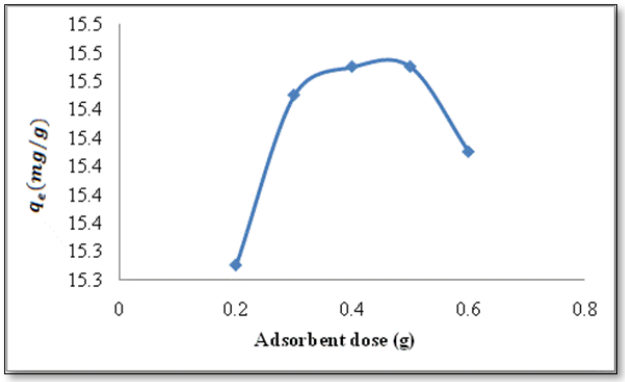

Figure 2. Variation of equilibrium amount of NR dye adsorbed with adsorbent dosage

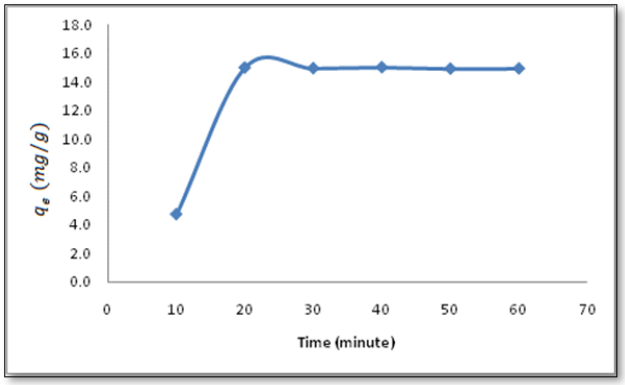

Figure 3. Variation of equilibrium concentration of NR dye adsorbed with time

Temperature also affected the extent of adsorption of NR dye unto wood saw dust. Temperature can affect adsorption in two ways. Firstly, the extent of adsorption may increase with increase in temperature leading to chemisorptions mechanism and secondly, the extent of adsorption can decrease with increase in temperature, which points toward physisorption mechanism.

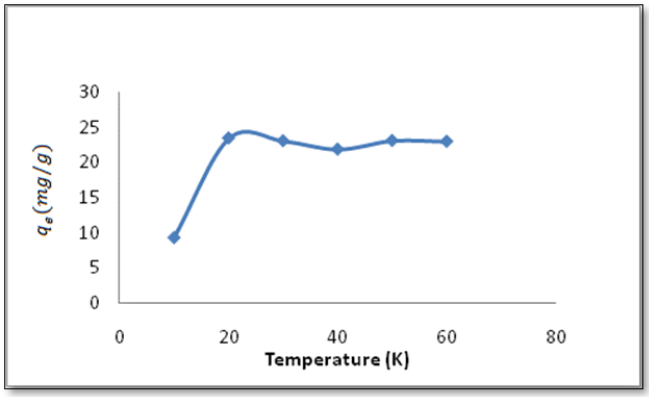

Figure 4. Variation of equilibrium amount of NR dye adsorbed with temperature

The adsorption of NR dye was found to support chemisorption mechanism, indicating that the equilibrium amount of dye adsorbed increased with increase in temperature and then remains constant after a certain temperature. The graph is shown in **Figure 5**.

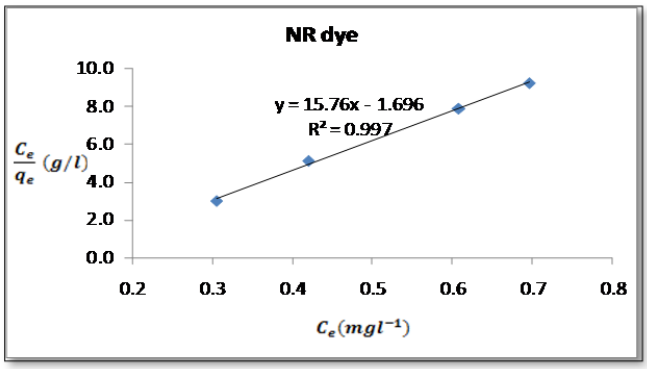

Figure 5. Langmuir isotherm for the adsorption of NR dye unto wood saw dust

ADSORPTION ISOTHERM

Adsorption isotherm gives the relationship between the amount of dye adsorbed with concentration at a given temperature. It is a unique factor that can be used to study the adsorption behavior of dyes and other adsorbates. Attempts to obtain best suited adsorption isotherm through fitting of data led to the conclusion that Langmuir, Temkin and Dubinin-Raduskevich isotherms best described the adsorption behavior of NR dye.

The Langmuir adsorption isotherm can be written according to equation 3 [16]

$$\frac{C_e}{q_e} = \frac{1}{q_m b} + \frac{C_e}{q_m} \qquad (3)$$

Where C_e is the equilibrium concentration of adsorbate (mg/l), q_e is the amount of adsorbate adsorbed per unit mass of the adsorbent (mg/l), b is the Langmuir adsorption

constant which is related to affinity between the adsorbate and the adsorbent while q_m is the theoretical monolayer saturation capacity. From the Langmuir equation, a plot of $\frac{C_e}{q_e}$ versus C_e should be liner if the Langmuir assumptions are valid. The Langmuir isotherm for the adsorption of NR dye unto wood saw dust are shown in **Figure 6**. The plot gave R^2 value of 0.997, which suggest an excellent degree of linearity. q_m and b values were 0.0206 mg/l and 0.7561 respectively. These values are comparable to those obtained for excellent adsorbents.

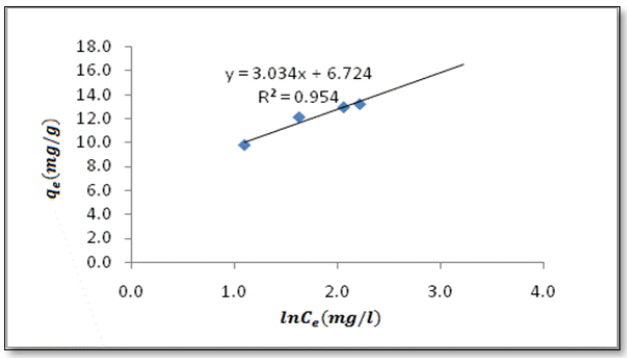

Figure 6. Temkin isotherm for the adsorption of NR dye

The Linear form of the Temkin isotherm can be written according to equation 4 [17]

$$q_e = BlnA + BlnC_e \quad (4)$$

Where: A is the Temkin isotherm constant (L/g), $B = RT/b$, b is the Temkin constant related to heat of sorption (J/mol), R is the gas constant (8.314 J/mol K), and T is the absolute temperature (K). Temkin adsorprion plot for the adsorption of NR dye unto wood saw dust is shown in **Figure 7**.

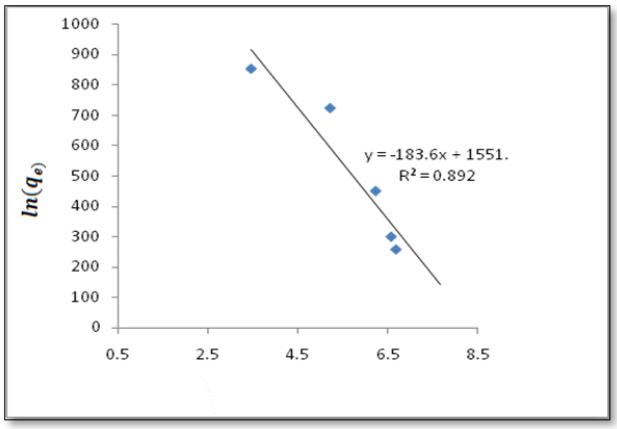

Figure 7. Dubinin-Raduskevich isotherm for the adsorption of NR dye unto wood saw dust

From the plot, Temkin adsorption constants (B = 3.034, ln A = 2.2162, b = 830.3039 and R^2 = 0.9540) were favorable and indicate excellent fitness of the adsorption process to the Temkin model.

The Dubinin-Radushkevich (DRK) adsorption model takes the form shown in equation 5 below

$$lnq_e = lnq_m - \beta\varepsilon^2 \quad (5)$$

where q_e is the equilibrium amount of the dye that is adsorbed (mg/g), q_m is the theoretical amount of dye adsorbed, β is the activity coefficient which is related to the mean sorption energy and ε is the Polanyl potential and can be expressed as,

$$\varepsilon = RTln\left(1 + \frac{1}{C_e}\right) \quad (6)$$

The value of the adsorption energy can be obtained from the following relation,

$$E_{ads} = \frac{1}{\sqrt{-2\beta}} \quad (7)$$

Application of the DRK equation requires that a plot of lnq_e versus ε^2 gives a straight line with slope equal to β and intercept equal to lnq_m. The DRK plots for the adsorption of NR dye unto wood saw dust is shown in **Figure 8.**

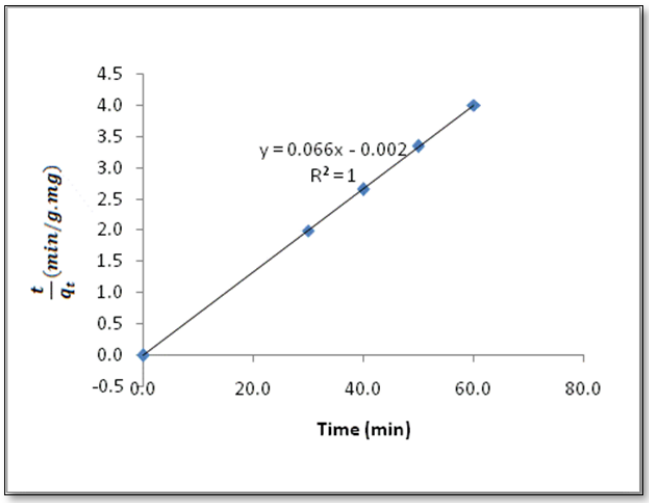

Figure 8. Pseudo second order kinetic plots for the adsorption of NR dye by wood sawdust

From the slope of the plots, the adsorption energy is 13.55 J/mol for NR dye. Generally, adsorption energy in the range of 1 to 8 kJ/mol point toward physiosorption while adsorption energy in the range of 8 to16 kJ/mol is an indication of chemisorptions. Therefore, NR dye is adsorbed unto wood saw dust through the mechanism of chemisorptions, as stated before.

KINETIC STUDY

In kinetic study of dye removal, two significant pseudo order models are pseudo first and pseudo second order kinetic models. The expressions for the models are provided in equations 4.6 and 4.7 respectively [18].

$$ln(q_e - q_t) = lnq_e - k_1 t \quad (8)$$

$$\frac{t}{q_t} = \frac{1}{k_2 q_e^2} + \frac{t}{q_e} \quad (9)$$

Curve fittings to kinetic models indicated that the adsorption of NR dye best agree with the pseudo second order kinetic (i.e equation 9). Therefore plots of $\frac{t}{q_t}$ versus t yielded straight as shown in **Figure 9**. Pseudo second order kinetic plot for the adsorption of NR dye unto wood saw dust is presented in **Figure 9**. The kinetic data is seen to fit the pseudo second order model excellently. Significant deduction that can be derived from the pseudo second order kinetic data is the initial adsorption rate (h) and half adsorption time ($t_{0.5}$) which can be expressed as $h = \frac{1}{k_2 q_e^2}$ and $t_{0.5} = \frac{1}{k_2 q_e}$ respectively. The results obtained in this study indicated that NR dye has good initial adsorption rate and half adsorption time.

Pseudo second order adsorption parameters obtained from the plot (Fig.8) were q_e (mg/g) = 166.67, k_2 = 0.0040 mol/s, h = 0.009, $t_{0.5}$ = 1.5000 and R^2 = 0.896.

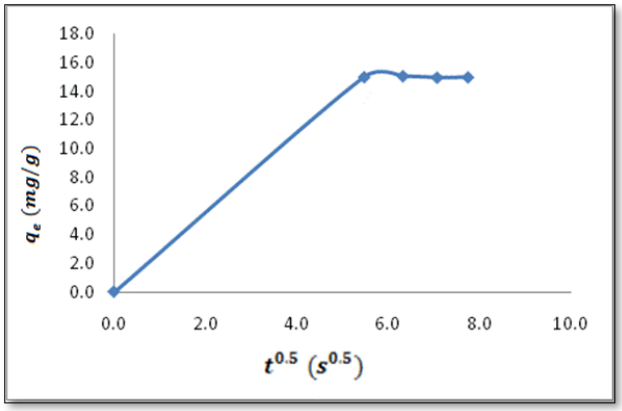

Figure 9. Intra particle diffusion plot fir the adsorption of NR dye unto wood saw dust

INTRA PARTICLE DIFFUSION MODEL

The existent of intra particle diffusion can be established if equation 10 is obeyed,

$$q_e = k_p t^{0.5} \quad (10)$$

Consequently, graph of q_e versus $t^{0.5}$ for the adsorption of NR dye (**Figure 10**) consisted of two sessions, which were a slowly rising graph and a linear section. The existent of non linear section in the plot indicates that both intra particle diffusion and surface adsorption occur simultaneously [15].

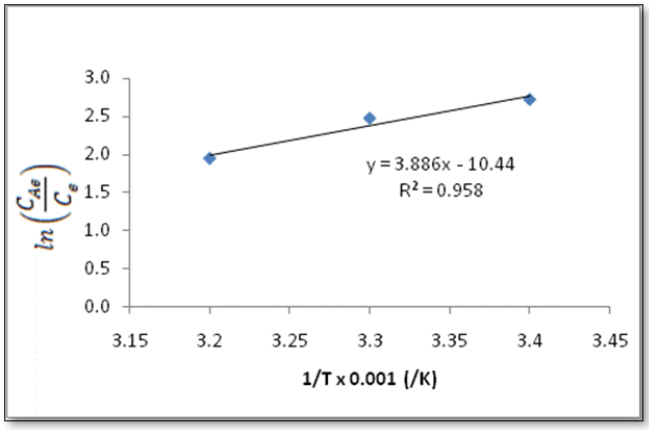

Figure 10. Variation of $ln\left(\frac{C_{Ae}}{C_e}\right)$ with 1/T for the adsorption of NR dye unto wood saw dust

THERMODYNAMIC STUDY

Thermodynamic adsorption parameter can be derived from the Gibb Helmholtz equation, which relates equilibrium constant with temperature [3],

$$\Delta G^0 = -RT\left(\frac{C_{Ae}}{C_e}\right) \quad (11)$$

Where R is the gas constant, T is the temperature, C_{Ae} is the solid phase concentration of the dye and C_e is the concentration of the dye in solution. Consequently, since $k_{eq} = \frac{C_{Ae}}{C_e}$, then,

$$ln\left(\frac{C_{Ae}}{C_e}\right) = \frac{\Delta S^0}{R} - \frac{\Delta H^0}{RT} \quad (12)$$

From equation 12, a plot of $ln\left(\frac{C_{Ae}}{C_e}\right)$ against 1/T is expected to be linear with slope and intercept corresponding to $\frac{\Delta H^0}{R}$ and. $\frac{\Delta S^0}{R}$ Estimated values of standard enthalpy change were 20.29 J/mol. However, values of standard entropy change were 82.10 J/mol. Therefore, the adsorption of NR dye is endothermic.

FTIR STUDY

FTIR spectrum of the dye

COMPUTATIONAL CHEMISTRY STUDY

Semi empirical indices are central for evaluating molecular reactivity, stability, electron donor-acceptor potentials and other electronic parameters associated with adsorption. Calculated semi empeirical parameters for NR dye were Total energy (-2802.55 eV), Electronic energy (-19389.344 eV), Core core repulsion (16586.79 eV), Cosmo area (283.88 $Å^2$), Cosmo volume (303.13 $Å^3$), ionization potential (8.19 eV), Energy of the HOMO (-8.19 eV), Energy of LUMO (-1.12 eV), Number of filled levels (48) and molecular weight (252.31 g/mol). These parameters compare favourable with data obtained for two dyes that were adsorbed effectively on ground nut shell surface [15].
Computational chemistry can be adequately used to predict or interpret the mechanism of adsorption or predict adsorption behavior of a given adsorbate or adsorbent [15]. Of great interest is the use of Fukui function, which enables the reactivity of a molecular species to be viewed in terms of the individual atoms that constitute the molecule. The Fukui functions for nucleophilic, electrophilic and radial attacks can be technically defined as follows [19],

$$f_x^+ = q_{N+1} - q_N \quad (13)$$

$$f_x^- = q_N - q_{N-1} \quad (14)$$

$$f_x^0 = \frac{[(q_{N+1}) - (q_{N-1})]}{2} \quad (15)$$

Whereq_N, q_{N+1} and q_{N-1} are the Mulliken charges of the molecule with N, N+1 and N-1 electrons respectively.

Fukui function analysis is based on the magnitude and sign of the calculated Fukui function (**Table 1**). The site that favors electrophilic attack is the site with the highest value of f_x^- while the site for nucleophilic attack is the site with the highest value of f_x^+. However, modern Fukui analysis requires that the site that has positive value for the difference between electrophilic and nucleophilic Fukui function will support nucleophilic attack and vice versa [20]. From both approaches, the possible sites for electrophilic attack are in the pyridine and enamine nitrogen (i.e N7, N10 and N15) **(Figure 11).**

Table 1. Huckel charges Fukui functions for nuclueophilic, electrophilic and radical attacks in NR dye.

Atom/No/type	Huckel charge	f_x^+	f_x^-	f_x^0	$f_x^+ - f_x^-$
C(1) Alkene	0.1480	15.0727	-15.1117	-0.0195	30.1844
C(2) Alkene	-0.1041	13.0747	-13.0951	-0.0102	26.1698
C(3) Alkene	-0.0451	1.9499	-1.9487	0.0006	3.8986
C(4) Alkene	0.0804	-3.9110	3.8907	-0.0102	-7.8017
C(5) Alkene	0.1351	-4.3749	4.3536	-0.0107	-8.7285
C(6) Alkene	-0.2241	4.4478	-4.5478	-0.0500	8.9956
N(7) Pyridine	-0.2805	-4.5251	4.6577	0.0663	-9.1828
C(8) Alkene	0.1340	-4.3655	4.3141	-0.0257	-8.6796
C(9) Alkene	0.1634	-4.3618	4.3151	-0.0233	-8.6769
N(10) Pyridine	-0.3871	-4.5576	4.6660	0.0542	-9.2236
C(11) Alkene	-0.0873	-3.8295	3.8342	0.0024	-7.6637
C(12) Alkene	0.0352	-3.9309	3.9106	-0.0101	-7.8415
C(13) Alkene	0.1801	-3.9979	3.9766	-0.0107	-7.9745
C(14) Alkene	-0.3103	-3.8239	3.8147	-0.0046	-7.6386
N(15) Enamine	0.0453	-5.1064	5.1088	0.0012	-10.2152
C(16) Alkane	-0.1108	-4.0340	4.0409	0.0034	-8.0749
N(17) Enamine	0.0643	7.6475	-7.8911	-0.1218	15.5386
C(18) Alkane	-0.0040	3.2431	-3.2052	0.0190	6.4483
C(19) Alkane	-0.0158	5.4213	-5.3768	**0.0222**	10.7981

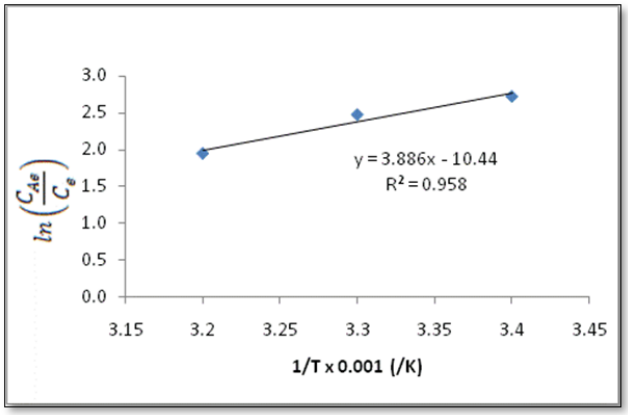

Figure 11. Variation of $ln\left(\frac{C_{Ae}}{C_e}\right)$ with 1/T for the adsorption of NR dye unto wood saw dust.

On the other hand, the sites for nucleophilic attack are in the alkene carbons (C1 and C2). This assertion is partly supported by values of calculated Huckel charged (which are also presented in Table 1) which uniquely identified the two pyridine nitrogen atoms (N7 and N10) as the two atoms that have the highest negative values of Huckel charge. Similarly, C9. C13 and C1 seems to have the highest positive values of Huckel charges, which suggest that the nucleophilic sites for attack resides along the benzene bonds surrounding this zone. The frontier molecular orbital theory of reactivity and selection suggests that electrophilic attack takes place in the HOMO and transfer electron from the HOMO to LUMO, which then facilitates adsorption [21]. The HOMO itself can be likened to electrophilic Fukui function while the LUMO should correspond to the nucleophic Fukui function. This approach is demonstrated in the HOMO and LUMO diagrams shown in Fig.11. In the diagram, green stands for negative while red stands for positive. It is clearly indicated in the diagram that the HOMO orbital is concentrated in the amine nitrogen (N7 and N10) while the LUMO orbital is concentrated in those atoms that has positive values of Δf. Adsorption involves either electron transfer (chemisorptions) or charge transfer (physiosorption) or both. Adsorption of NR dye unto wood saw dust proceded predominantly through the mechanism of chemisorptions, therefore, electron transfer from charge NR molecule to charged saw dust surface must have facilitated the adsorption process [15].

Molecular mechanics analysis indicated that the amine nitrogen (N7 and N10) has one lone pair of electrons each, hence it can donate the electron to a vacant orbital in the adsorbent and this enhances adsorption **(Figure 12 and 13)**. Nitrogen is a hetero atom, known for its strong tendency to facilitate adsorption through electron donation [22-25].

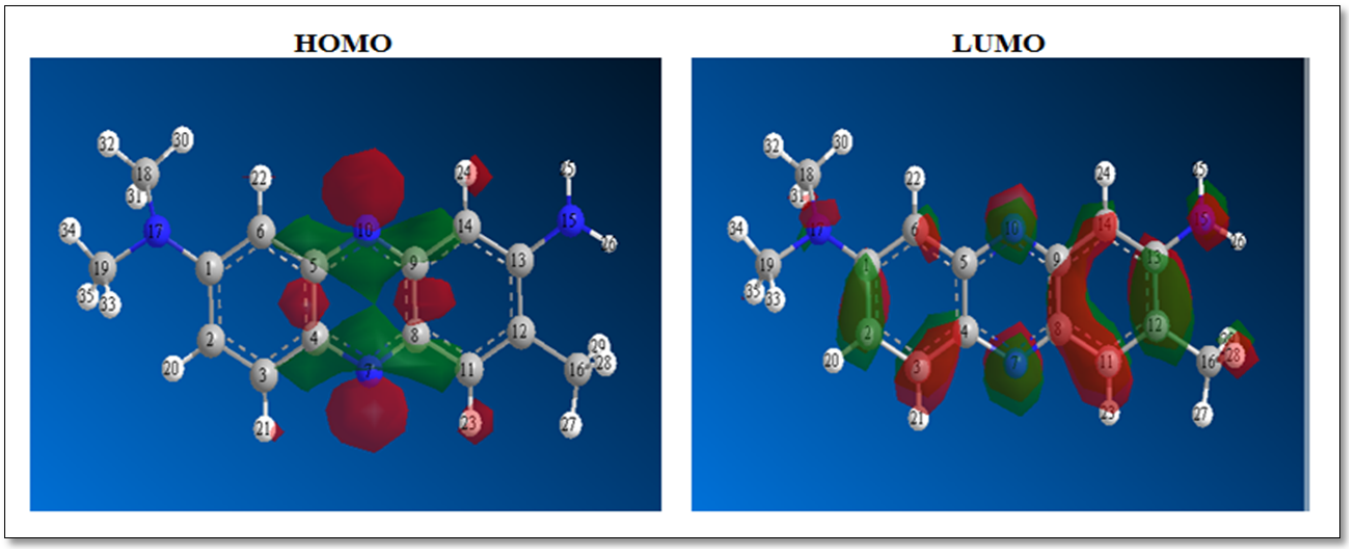

Figure 12. 3-D structure of NR dye showing HOMO and LUMO locations.

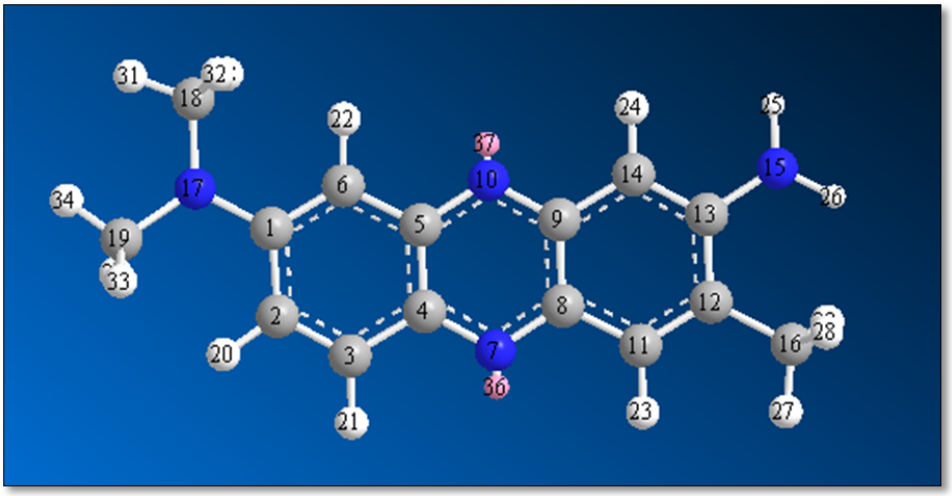

Figure 13. 3D structure of NR dye showing lone pair electrons on the pyridine nitrogen atoms (LP (36) and LP (37).

CONCLUSION

The experimental results obtained from this study qualify *Musanga cecropioides* saw dust is a good adsorbent for the removal of dye from aqueous solution. The adsorbent functions through mechanism of adsorption and displayed mono layer adsorption model, best described by Langmuir, Temkin and Dubinin-Radushkevich isotherms. The adsorption performance of wood saw dust vary with the period of contact, temperature, adsorbent dosage and concentration. A close examination of these parameters as well as established kinetic and thermodynamic models can provide relevant information in improving the adsorption efficiency of the wood saw dust.

REFERENCES

1. EPA (2018) Drinking water standard and health advisory table. Office of water, US, Environmental Protection Agency, Washington.

2. Sarkheil H, Noormohammadi F, Rezaei AR, Borujeni MK (2014) Dye pollution removal from mining industrial wastewaters using chitosan nanoparticles. Proceeding of International conference on Agriculture, Environmental and Biological Sciences. Held in Antalya (Turkey), pp: 37-42.

3. Kumar PS, Fernando PSA, Ahmed RT, Srinath R, Priyadharshini M, et al. (2013) Effect of temperature on the adsorption of methylene blue dye onto sulfic acid-treated orange peel. Chem Eng Commu 201: 1526-1547.

4. Banerjee S, Chattopadhyaya MC, Srivastava V, Sharma Y (2014) Adsorption studies of methylene blue onto activated saw dust: Kinetics, equilibrium and thermodynamic studies. Environ Prog 33: 790-799.

5. Castro MFA, Abad MLB, Sumalinog DAO, Abarea RRM, Paoprasert P, et al. (2018) Adsorption of methylene blue dye and Cu(II) ions on EDTA-modified bentoniite: Isotherm, kinetic and thermodynamic studies. Sustain Environ Res 28: 197-205.

6. Iqbal M, Aftab AK, Nazil ZH, Bhatti HN, Nouren S (2018) Dyes adsorption using clay and modified clay: A review. J Mol Liq 256: 395-407.

7. Yagub MT, Sen TK, Afoze S, Ang HM (2013) Dye and its removal from aqueous solution by adsorption: A review. Adv Colloid Interface Sci 209: 172-184.

8. Ngulube T, Gumbo JR, Masindi V, Maity A (2017) An update on synthetic dyes adsorption onto clay-based minerals: A state-of-art review. J Environ Manag 191: 35-57.

9. Chaari I, Fakhfakh F, Medhioub M, Jamoussi F (2019) Comparative study on adsorption of cationic and anionic dyes by smectite rich natural clays. J Mol Struct 1179: 672-67.

10. Aboelenin R, Kheder S, Farag H, El Nabarawy T (2017) Removal of cationic neutral red dye from aqueous solutions using natural and modified rice straw. Egypt J Chem 60.

11. Lei DY, Li B, Wang Q, Wu B, Ma L, et al. (2015) Removal of neutral red from aqueous solution using Pleurotus ostreatus nanoparticles by response surface methodology. Desalin Water Treat 54: 2794-2805.

12. Zhang L, Tu L, Liang Y, Chen Q, Li Z, et al. (2018) Coconut-based activated carbon fibers for efficient

adsorption of various organic dyes. RSC Adv 74: 42280-42288.

13. Iram M, Guo C, Guan Y, Ishfaq A, Liu H (2010) Adsorption and magnetic removal of neutral red dye from aqueous solution using Fe3O4 hollow nanospheres. J Harzad Mater 181: 1039-1050.

14. Zou W, Bai H, Gao S (2012) Competitive adsorption of neutral red and Cu2+ onto pyrolytic char: Isotherm and kinetic study. JCE 57: 2792-2801.

15. Eddy NO, Ekwememgbo P, Odoemelam SA (2008) Inhibition of the corrosion of mild steel in H2SO4 by 5-amino-1-cyclopropyl-7-[3R-5S)-3,5-dimethylpiperazin-1yl)-6,8-difluoro-4-oxo-quinoline-3-carboxylix acid (ACPDQC). Int J Phys Sci 3: 275-280.

16. Odoemelam SA, Eddy NO (2009) Studies on the use of oyster, snail and periwinkle shells as adsorbents for the removal of Pb2+ from aqueous solution. E. J Chem 6: 213-222.

17. Eddy NO (2009) Modeling of the adsorption of Zn2+ from aqueous solution by modified and unmodified Cyperus esculentus shell. Elec J Environ Agric Food Chem 8: 1177-1185.

18. Simoni J (2016) Comparison of Pseudo first order and pseudo second rate laws in the modeling of adsorption kinetics. Chem Eng J 300: 254-263.

19. Eddy NO, Essien NB (2017) Computational chemistry study of toxicity of some m-tolyl acetate derivatives insecticides and molecular design of structurally related products. In Silico Pharmacol 5: 14.

20. Eddy NO, Awe FE (2018) Experimental and quantum chemical studies on ethanol extract of Phyllanthus amarus (EEPA) as a green corrosion inhibitor for aluminium in 1 M HCl. Port Electrochimica Acta 36: 231-247.

21. Eddy NO, Ibok UJ, Ameh PO, Alobi NO, Sambo MM (2014) Adsorption and quantum chemical studies on the inhibition of the corrosion of aluminum in HCl by Gloriosa superba (GS) gum. Chem Eng Commun 201: 1360-1383.

22. Ameh PO, Eddy NO (2018) Experimental and Computatonal Chemistry studies on the inhibition efficiency of phthalic acid (PHA) for the corrosion of aluminum in hydrochloric and tetraoxosulphate (VI) acids. Prot Met Phys Chem Surf 54: 1169-1181.

23. Badu M, Boatend IW, Boa NO (2019) Evaluation of adsorption of textile dyes by wood sawdust. Res J Phys Appl Sci 3: 006-014.

24. Eddy NO, Awe EE, Ebenso EE (2010a) Adsorption and inhibitive properties of ethanol extracts of leaves of Solanum melongena for the corrosion of mild steel in 0.1 M HCl. Int J Electrochem Sci 5: 1996-2011.

25. Eddy NO, Odiongenyi AO (2010b) Corrosion inhibition and adsorption properties of ethanol extract of Heinsacrinata on mild steel in H2SO4. Pigm Resin Technol 39: 288-295.